THE JOURNAL OF BIOLOGICAL CHEMISTRY VOL. 283, NO. 42, pp. 28741–28746, October 17, 2008

Three Metal Ions Participate in the Reaction Catalyzed by T5 Flap Endonuclease*[S]

Received for publication, February 15, 2008, and in revised form, August 7, 2008 Published, JBC Papers in Press, August 11, 2008, DOI 10.1074/jbc.M801264200

Karl Syson[‡1], Christopher Tomlinson[‡], Brian R. Chapados[§], Jon R. Sayers[¶], John A. Tainer[§], Nicholas H. Williams[‡], and Jane A. Grasby[‡2]

From the [‡]Department of Chemistry, Centre for Chemical Biology, Krebs Institute, University of Sheffield, Sheffield S3 7HF, United Kingdom, the [¶]Henry Wellcome Laboratories for Medical Research, University of Sheffield School of Medicine and Biomedical Science, Sheffield S10 2RX, United Kingdom, and the [§]Department of Molecular Biology, Skaggs Institute for Chemical Biology, The Scripps Research Institute, La Jolla, California 92037

Protein nucleases and RNA enzymes depend on divalent metal ions to catalyze the rapid hydrolysis of phosphate diester linkages of nucleic acids during DNA replication, DNA repair, RNA processing, and RNA degradation. These enzymes are widely proposed to catalyze phosphate diester hydrolysis using a "two-metal-ion mechanism." Yet, analyses of flap endonuclease (FEN) family members, which occur in all domains of life and act in DNA replication and repair, exemplify controversies regarding the classical two-metal-ion mechanism for phosphate diester hydrolysis. Whereas substrate-free structures of FENs identify two active site metal ions, their typical separation of >4 Å appears incompatible with this mechanism. To clarify the roles played by FEN metal ions, we report here a detailed evaluation of the magnesium ion response of T5FEN. Kinetic investigations reveal that overall the T5FEN-catalyzed reaction requires at least three magnesium ions, implying that an additional metal ion is bound. The presence of at least two ions bound with differing affinity is required to catalyze phosphate diester hydrolysis. Analysis of the inhibition of reactions by calcium ions is consistent with a requirement for two viable cofactors (Mg^{2+} or Mn^{2+}). The apparent substrate association constant is maximized by binding two magnesium ions. This may reflect a metal-dependent unpairing of duplex substrate required to position the scissile phosphate in contact with metal ion(s). The combined results suggest that T5FEN primarily uses a two-metal-ion mechanism for chemical catalysis, but that its overall metallobiochemistry is more complex and requires three ions.

Key cellular processes such as DNA replication, DNA repair, RNA processing, and RNA degradation require the rapid hydrolysis of the phosphate diester linkages of nucleic acids. The uncatalyzed hydrolysis of phosphate diesters under biological conditions is an extremely slow process with an estimated half-life of 30 million years at 25 °C (1). Protein nucleases and RNA enzymes produce rate enhancements of 10^{15}–10^{17} to allow this reaction to proceed on a biologically useful time scale. Most enzymes catalyzing phosphate diester bond hydrolysis have a requirement for divalent metal ions. Based largely upon crystallographic observations, most metallonucleases are proposed to catalyze reactions using a two-metal-ion mechanism (Fig. 1*a*) analogous to that suggested for the phosphate monoesterase alkaline phosphatase (2, 3), although this view is not universally accepted. Three recent reviews present contrasting views on the roles of metal ions in protein nuclease and RNA enzyme reactions and illustrate this controversy (4–6).

One family of metallonucleases over which there has been considerable mechanistic debate are the flap endonucleases (FENs)[3] (7–12), which are present in all domains of life and play a key role in DNA replication and repair. Unlike most metallonucleases, which typically possess a cluster of three or four active site carboxylates, the FEN active site is constructed from seven or eight acidic residues located in similar positions in FENs from a range of organisms (Fig. 1*b*, see also supplemental Fig. S1) (7, 9, 10, 13–16). Several FEN x-ray structures also contain two active site carboxylate-liganded divalent metal ions, designated as metals 1 and 2 (9, 13–15). The position of metal 1 is similar in all cases, but the metal 2 location varies. In all but one structure of human FEN (hFEN), the spacing of these metal ions exceeds that demanded by a two-metal-ion mechanism, which needs to be ≤4 Å for the two ions to bind the same oxygen atom (Fig. 1*a*). Only two structures of enzyme-DNA complexes exist, but neither contain bound metal ions (8, 17).

To investigate the roles played by metal ions in the FEN reaction, we have carried out a detailed evaluation of the magnesium ion response of T5FEN, and of the inhibition of magnesium- and manganese ion-supported reactions by calcium ions. Together the data suggest that the major acceleration of phosphate diester hydrolysis requires at least two viable cofactor ions, and so could utilize a two-metal-ion mechanism, but that the metallobiochemistry of T5FEN is more complex and overall involves at least three metal ions.

* This work was supported, in whole or in part, by National Institutes of Health Grant CA081967 (to J. A. T.) and SBDR Program Grant P01 CA92584 (to J. A. T.). This work was also supported by BBSRC Grants B20079 and F0147321 (to J. A. G. and N. H. W.). The costs of publication of this article were defrayed in part by the payment of page charges. This article must therefore be hereby marked "*advertisement*" in accordance with 18 U.S.C. Section 1734 solely to indicate this fact.

[S] The on-line version of this article (available at http://www.jbc.org) contains supplemental Figs. S1–S4.

[1] Current address: John Innes Centre, Norwich Research Park, Colney, Norwich NR4 7UH, UK.

[2] To whom correspondence should be addressed: Centre for Chemical Biology, Dept. of Chemistry, Krebs Institute, University of Sheffield, Sheffield, S3 7HF, UK. Tel.: 441142229478; Fax: 441142229346; E-mail: j.a.grasby@sheffield.ac.uk.

[3] The abbreviations used are: FEN, flap endonuclease; MOPS, 4-morpholinepropanesulfonic acid; CHES, 2-(cyclohexylamino)ethanesulfonic acid.

EXPERIMENTAL PROCEDURES

Materials—T5FEN was purified to homogeneity as described (18). HP5F substrate (5′-FAM-pd(CGCTGTCGAACA-CACGCTTGCGTGTGTTC)) was prepared as described (19) and after purification, divalent metal ion contaminants were removed by treatment with Chelex resin. ICP mass spectrometry was used to confirm the absence of significant divalent metal ion contamination in all materials.

Steady State Kinetic Analyses—Steady state kinetic parameters of T5FEN were evaluated at 37 °C using HP5F substrate in 25 mM CHES or potassium glycinate, pH 9.3, 0.1 mg/ml bovine serum albumin, and 1 mM dithiothreitol as described (19). $MgCl_2$ was added to the desired concentration and the ionic strength ($MgCl_2$ + KCl) adjusted to 80 mM using KCl. Substrate concentrations were varied around the K_m, and reactions were sampled and quenched by addition of an equal volume of 25 mM EDTA at appropriate time intervals. Reactions were analyzed by dHPLC equipped with a fluorescence detector and initial rates (v) were calculated as described (19). Steady state catalytic parameters were determined at each Mg^{2+} concentration by curve fitting to the Michaelis-Menten equation. Plots of v/[E] *versus* [S], where [S] $\ll K_m$ and 29[S] $\leq$ [Mg^{2+}]/10 were also used to determine k_{cat}/K_m.

Calcium Inhibition—Reaction mixtures containing 0.1 or 2 mM $MgCl_2$, HP5F (3 or 1 μM, respectively), 25 mM potassium glycinate, pH 9.3, 0.1 mg/ml bovine serum albumin, appropriate amounts of T5FEN (400–1500 pM), and varying $CaCl_2$ with the appropriate amount of KCl to maintain the same ionic strength in all experiments, were used to determine the initial rate of reaction in the presence of Ca^{2+}. For manganese-supported reactions, reaction mixtures contained 100 μM $MnCl_2$, 100 nM HP5F, 25 mM MOPS, pH 7.5, 0.1 mg/ml bovine serum albumin, 200–1500 pM T5FEN, and $CaCl_2$ with the appropriate amount of KCl. Reactions were analyzed as above to determine k_{obs} ($k_{obs} = v$/[E]) as a function of calcium ion concentration.

Curve Fitting—All curve fitting was carried out by non-linear regression fitting using Kaleidagraph software (Synergy Software, Reading, PA) where appropriate weighted according to individual error values, using Equations 1–7 (see "Results").

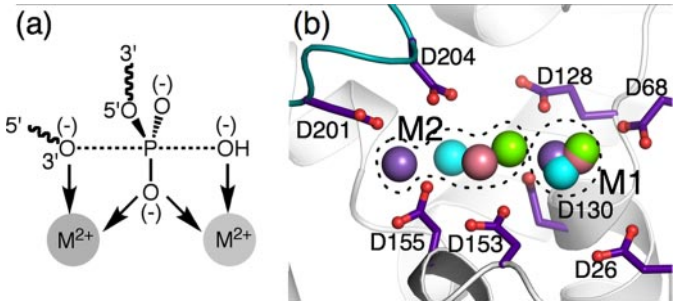

FIGURE 1. **The two-metal-ion mechanism proposed for reactions of metallonucleases and the active site of T5FEN showing the varying positions of metal ions in FEN structures.** *a*, two metal-ion mechanism. One metal ion acts as a source of nucleophilic hydroxide ion and binds to a non-bridging oxygen of the scissile phosphate diester acting as an electrophilic catalyst. A second metal ion is coordinated to the leaving group oxygen assisting with leaving group departure and binds to the same non-bridging oxygen of the scissile phosphate diester. *b*, active site structure of T5FEN (1UT5, *gray with purple* carboxylate residues) illustrating the loop of the helix-three-turn-helix (H3TH) (teal) motif and seven active site carboxylates present in similar positions in all FENs and the eighth carboxylate (*D201*) present in the active sites of bacteriophage and bacterial enzymes (see supplemental Fig. S1). Two metal ions, M1 and M2 (*purple*) are bound with a separation of 8 Å. Metal ions observed in structures of T4FEN (1TFR, *cyan*), MjFEN (*Methanococcus jannaschii,* 1A77, *rose*), hFEN (1UL1x, *green*), positioned by overlay, are shown. Although all FENs conserve seven active site carboxylates, the position of M2 observed in each structure is variable.

RESULTS

Stimulation of FEN Catalysis by Magnesium Ions—To elucidate the role and minimal number of metal ions involved in the T5FEN-catalyzed reaction, kinetic parameters were monitored as a function of magnesium ion concentration. As the concentration of Mg^{2+} was varied, the ionic strength of reaction mixtures was kept constant by adjusting the amount of potassium chloride present. A fluorescent 29 nucleotide 5′-overhanging DNA hairpin substrate (HP5F) was employed. The characteristics of the T5FEN-catalyzed reaction of HP5F have been reported previously (19–21). As both maximal steady state and single turnover rates of Mg^{2+}-supported reactions reach a pH-independent plateau above pH 8.5, pH 9.3 was selected as the pH optimum for the experiments. The variations of the individual kinetic parameters with magnesium ion concentration are shown in Fig. 2, *a*–*c*, and sample individual experiments are shown as supplemental Fig. S2.

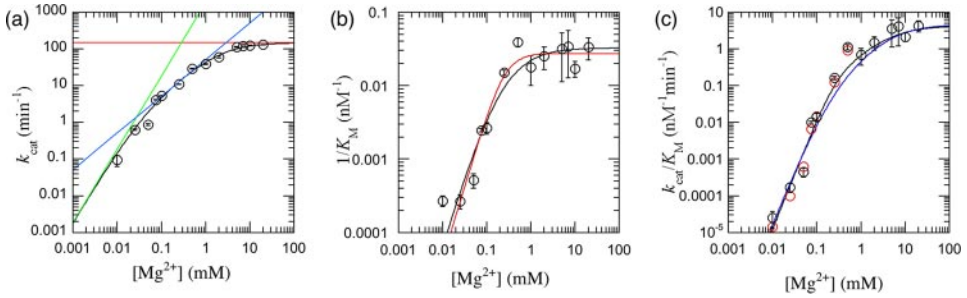

FIGURE 2. **Variation of the steady state catalytic parameters of T5FEN as a function of magnesium ion concentration.** Experiments were conducted at pH 9.3 and 37 °C with varying amounts of $MgCl_2$ and KCl to maintain constant ionic strength. All measurements represent the result of three independent experiments with standard errors shown. *a*, variation in k_{cat} as a function of magnesium ion concentration. Slopes of 0 (*red*), 1 (*blue*), and 2 (*green*) are illustrated. The data have been fit to Equation 2 ("Results"), yielding $K_{DMgES1} = 0.04 \pm 0.003$ mM and $K_{DMgES2} = 2.3 \pm 0.06$ mM and $(k_{cat})_{max} = 146 \pm 1$ min^{-1}. *b*, variation in $1/K_m$ as a function of magnesium ion concentration fitted to Equation 3 with $K_{DMgE1} = K_{DMgE2}$ (*black curve*, yields $K_{DMgE1} = K_{DMgE2}$ 0.22 ± 0.02 mM and $(1/K_m)_{max} = 0.03 \pm 0.003$ nM^{-1}) and Equation 4 where $n = 2$ (*red curve*, yields $K^2_{DMgE} = 0.07 \pm 0.007$ mM^2, and $(1/K_m)_{max} = 0.03 \pm 0.003$ nM^{-1}). *c*, variation in k_{cat}/K_m for as a function of magnesium ion concentration fitted to Equation 5 with $K^2_{DMgE} = 0.07$ mM^2 (*black curve*, yields $K_{DMgE2} = 4.9 \pm 1.4$ mM and $(k_{cat}/K_m)_{max} = 4.2 \pm 1$ min^{-1} nM^{-1}) and Equation 6 with $K_{DMgE1} = K_{DMgE2} = 0.21$ mM (*blue curve*, yields $K_{DMgE3} = 6.0 \pm 1.8$ mM and $(k_{cat}/K_m)_{max} = 4.6 \pm 1.3$ min^{-1} nM^{-1}). Data shown as *black circles* are derived from the individual catalytic parameters whereas data shown as *red circles* are the observed rate constant at low concentrations of substrate where 29[S] < [Mg]/10.

The turnover number (k_{cat}) is magnesium ion-dependent and increases until a Mg^{2+}-independent plateau is observed above 10 mM. Below 10 μM Mg^{2+}, reactions no longer proceed to completion, and therefore data were not collected below this concentration. At low magnesium ion concentration (10–

100 μM), k_{cat} has a second order dependence on divalent metal ion concentration (Fig. 2*a*, *green* slope of 2 in log-log plot) that becomes first order (Fig. 2*a*, *blue* slope of 1) at cofactor concentrations greater than 100 μM. This change in reaction order cannot be accounted for by the participation of a single Mg^{2+} in the FEN-catalyzed reaction (see Equation 1). A reaction supported by a single ion would display first order dependence (Fig. 2*a*, slope of 1 in log-log plot) at all concentrations of magnesium ions $\leq K_{DMgES}$. Instead the minimal number of metal ions that could give rise to the behavior observed in Fig. 2*a* is 2. Moreover the change in reaction order requires that these two metal ions are bound independently and have differing affinities, but that for a reaction to proceed, both ions must be present. A model of this situation leads to Equation 2, where $(k_{cat})_{obs}$ is the observed turnover number at a given concentration of magnesium ions, K_{DMgES1} and K_{DMgES2} are the respective apparent magnesium ion dissociation constants from the ES complex, and $k_{cat(max)}$ is the maximal turnover rate at infinite magnesium ion concentration. At low concentrations of metal ions ([Mg] $< K_{DMgES1}$ and K_{DMgES2}), two metal ion binding sites of differing affinity need to be occupied to produce a catalytically active form of the enzyme giving rise to the slope of 2. At higher concentrations of magnesium ions ([Mg] $< K_{DMgES2}$ but [Mg] $> K_{DMgES1}$, so that (K_{DMgES1} + [Mg]) = [Mg]), the higher affinity site is saturated, and the reaction becomes first order as only the low affinity site is titrated and the occupancy of both sites is necessary for reaction to proceed. Curve fitting of the data to Equation 2 yields metal ion dissociation constants of $K_{DMgES1} = 0.04 \pm 0.003$ mM and $K_{DMgES2} = 2.25 \pm 0.06$ mM.

$$(k_{cat})_{obs} = \frac{(k_{cat})_{max}[Mg^{2+}]}{K_{DMgES} + [Mg^{2+}]} \quad \text{(Eq. 1)}$$

$$(k_{cat})_{obs} = \frac{(k_{cat})_{max}[Mg^{2+}]^2}{(K_{DMgES1} + [Mg^{2+}])(K_{DMgES2} + [Mg^{2+}])} \quad \text{(Eq. 2)}$$

Product release is partially rate-limiting for T5FEN-catalyzed hydrolysis of HP5F (22). Thus, the rate constants under single turnover conditions (k_{ST}) were also monitored as a function of magnesium concentration, and are 2–3-fold greater than k_{cat} in all cases (supplemental Fig. S3). The response to magnesium ion concentration is the same as for the k_{cat} data and could be fitted to Equation 2 to give K_{DMgES1} and K_{DMgES2} values of 0.09 ± 0.01 mM and 2.8 ± 0.35 mM, respectively. These values are in good agreement with those obtained from the k_{cat} data, and so the parameters obtained from Fig. 2*a* apply to the magnesium-dependent events prior to product release.

HP5F binds to T5FEN weakly in the absence of divalent metal ions ($K_D > 15$ μM). Substrate/product binding equilibria, as reflected by $1/K_m$, are magnesium ion-dependent and K_m reaches a minimum (0.04 ± 0.01 μM) above 0.25 mM Mg^{2+} (Fig. 2*b*). In the Mg^{2+}-dependent range, the slope of the log-log plot is 1.8 ± 0.2, suggesting a second order dependence. This magnesium-dependent behavior can only be explained by the involvement of at least two metal ions, but could potentially arise from two different models. In one model, two metal ions bind independently, and the presence of both is required to stabilize one or more enzyme-substrate state(s). However, to give rise to the slope close to 2 over the whole Mg^{2+}-dependent range, both metal ions must bind with virtually identical binding constants. Applying this model to the data (Equation 3, where $(1/K_m)_{obs}$ is the observed parameter at a given magnesium ion concentration, $(1/K_m)_{max}$ is the maximal reciprocal of the concentration of substrate required to convert half the enzyme into the form(s) preceeding the rate-limiting step(s) at infinite magnesium ion concentration, and K_{DMgE1} and K_{DMgE2} are the respective apparent magnesium ion dissociation constants from free enzyme, with K_{DMgE1} and K_{DMgE2} kept identical) yields values of K_{DMgE1} (= K_{DMgE2}) = 0.21 ± 0.02 mM (Fig. 2*b*).

$$\left(\frac{1}{K_m}\right)_{obs} = \frac{\left(\frac{1}{K_m}\right)_{max}[Mg^{2+}]^2}{(K_{DMgE1} + [Mg^{2+}])(K_{DMgE2} + [Mg^{2+}])} \quad \text{(Eq. 3)}$$

In an alternative model, the metal ions bind cooperatively to the enzyme. A curve fit to this scheme (Equation 4, $n = 2$, where K^2_{DMgE} is the product of 2 apparent magnesium ion dissociation constants from free enzyme) yields $K^2_{DMgE} = 0.07 \pm 0.01$ mM^2. The difference between independent and cooperative behavior is only evident as the curves approach saturation, where an independent binding model produces a more gradual change to metal ion-independent behavior (see Fig. 2*b*). Distinguishing between these two models is generally difficult and especially so for this data set because K_m measurements for nucleases derived from discontinuous assays are typically associated with errors of $\pm$30%.

$$\left(\frac{1}{K_m}\right)_{obs} = \frac{\left(\frac{1}{K_m}\right)_{max}[Mg^{2+}]^n}{K^n_{DMgE} + [Mg^{2+}]^n} \quad \text{(Eq. 4)}$$

The magnesium ion dependence of the overall FEN reaction (k_{cat}/K_m) is shown in Fig. 2*c*. The apparent second order rate constant can be obtained in two ways, either from the individual catalytic parameters reported above, or as the gradient of a plot of v/[E] *versus* [S] at concentrations of [S] $\ll K_m$. Both of these approaches produce identical data within experimental error (Fig. 2*c*). In the latter case, the total concentration of phosphate diesters in HP5F was equal to or lower than 10% of the concentration of Mg^{2+}, ruling out the possibility that Mg^{2+} binding to HP5F is affecting the cofactor dependence. The apparent second order rate constant increases with magnesium concentration, reaching a Mg^{2+}-independent plateau above 2 mM. Importantly, the slope of the log-log plot at low Mg^{2+} concentrations is 2.9 ± 0.2, requiring the participation of at least three metal ions. As with the $1/K_m$ data, either independent binding or cooperative models could explain the behavior. Furthermore, as this is at least a three-ion process, combinations of independent and cooperative models are plausible. All of these models fit the data reasonably. To maintain consistency with the data derived from the individual catalytic parameters, a combination of cooperative and independent binding models (Equation 5) with $K^2_{DMgE2} = 0.07$ mM^2 produces a convincing data fit and a value for the dissociation constant of the

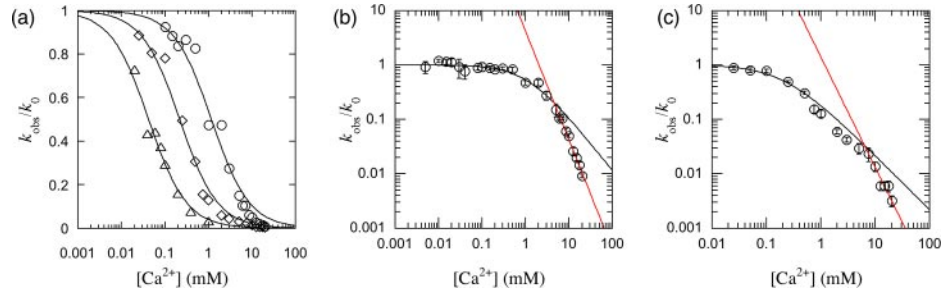

FIGURE 3. **The inhibitory effects of added calcium ions on Mg^{2+}- and Mn^{2+}-supported T5FEN reactions.** Experiments were conducted at 37 °C with varying amounts of $CaCl_2$ and KCl to maintain the same ionic strength in all experiments. Reactions supported by Mg^{2+} were studied at pH 9.3, whereas those supported by Mn^{2+} were studied at pH 7.5 as described under "Experimental Procedures." *a*, variation in k_{obs}/k_0 as a function of calcium ion concentration where k_{obs} is the observed normalized initial rate (v/[E]) at a given concentration of Ca^{2+} and k_0 is v/[E] in the absence of Ca^{2+}. Reactions contained 0.1 mM Mg^{2+} (*triangles*), 2 mM Mg^{2+} (*diamonds*), or 0.1 mM Mn^{2+} (*circles*). Data were fitted to Equation 7 to yield respective values of apparent K_i (the concentration of Ca^{2+} where $k_{obs}/k_0 = 0.5$) of 0.037 ± 0.002 mM, 0.22 ± 0.02 mM, and 1.2 ± 0.1 mM. *b*, the variation in k_{obs}/k_0 as a function of Ca^{2+} concentration for a reaction containing 0.1 mM Mn^{2+}. Combined standard errors for k_{obs}/k_0 are shown. The *black line* shows the best fit to a simple competitive inhibition scheme where one Ca^{2+} displaces one Mn^{2+} (Equation 7). The *red line* is a slope of −2 indicating a dependence on $1/[Ca^{2+}]^2$ at high Ca^{2+}. *c*, variation in k_{obs}/k_0 as a function of Ca^{2+} concentration for a reaction containing 2 mM Mg^{2+}. Combined standard errors for k_{obs}/k_0 are shown. The *black line* shows the best fit to Equation 7. The *red line* is a slope of −2 indicating a dependence on $1/[Ca^{2+}]^2$ at high Ca^{2+}.

third magnesium ion from the enzyme of 4.9 ± 1.4 mM (K_{DMgE3}). If the independent binding model is used (Equation 6 with $K_{DMgE1} = K_{DMgE2} = 0.21$ mM), $K_{DMgE3} = 6.1 \pm 1.8$ mM.

$$\left(\frac{k_{cat}}{K_m}\right)_{obs} = \frac{\left(\frac{k_{cat}}{K_m}\right)_{max}[Mg^{2+}]^3}{(K_{DMgE}^2 + [Mg^{2+}]^2)(K_{DMgE3} + [Mg^{2+}])} \quad \text{(Eq. 5)}$$

$$\left(\frac{k_{cat}}{K_m}\right)_{obs} = \frac{\left(\frac{k_{cat}}{K_m}\right)_{max}[Mg^{2+}]^3}{(K_{DMgE1} + [Mg^{2+}])(K_{DMgE2} + [Mg^{2+}])(K_{DMgE3} + [Mg^{2+}])} \quad \text{(Eq. 6)}$$

One caveat on the interpretation of this and any metal ion titration data is that the experiments only report on the presence and affinity of magnesium ions in the tested data range. If one or more metal ions are tightly bound over the entire range allowing data collection, then the total number of metal ions required to support the overall catalytic process is 4 or more.

Inhibition of FEN Catalysis by Calcium Ions—When supplied as the sole cofactor, calcium ions do not support FEN catalysis. However, as is typical for other divalent metal ion-dependent nucleases, Ca^{2+} ions have been demonstrated to stabilize protein-DNA interactions in the absence of catalytically viable cofactors (12). To investigate the effect of added calcium ions on the Mg^{2+}-supported FEN reaction, the rate of reaction was measured as a function of Ca^{2+} concentration at pH 9.3 in the presence of subsaturating Mg^{2+}, but with saturating HP5F. The effects of addition of calcium ions on the Mn^{2+}-supported FEN reaction were also investigated. For Mn^{2+}-supported reactions, the pH was reduced to 7.5 to avoid the problems associated with the formation of manganese hydroxides at higher pH values. This pH value is still above the measured pK_a for the Mn^{2+}-supported FEN-catalyzed reaction of HP5F (21). All reactions were inhibited by addition of Ca^{2+} (Fig. 3). To evaluate the apparent K_i at a given concentration of cofactor, data were fitted to a simple competitive inhibition model (Equation 7) where k_{obs} is the normalized initial rate (v/[E]) at a given concentration of calcium ions, k_0 is v/[E] in the absence of calcium ions, and K_i is equal to the concentration of calcium ions that produces 50% inhibition at the respective concentration of viable divalent metal ion cofactor. In all cases, the data fit acceptably to a simple competitive inhibition model up to 80% inhibition ($k_{obs}/k_0 = 0.2$) (Fig. 3*a*). At 2 mM Mg^{2+} $K_i = 0.22 \pm 0.02$ mM whereas decreasing the concentration of Mg^{2+} to 0.1 mM decreased $K_i = 0.037 \pm 0.002$ mM, indicating that Ca^{2+} inhibition is competitive with Mg^{2+}. At 0.1 mM Mn^{2+} the $K_i = 1.2 \pm 0.1$ mM. The 30-fold higher concentration of Ca^{2+} ions required to inhibit the Mn^{2+} reaction by a factor of 2 may in part be a consequence of the greater affinity of the FEN protein for Mn^{2+} *versus* Mg^{2+} (12, 21). However, by necessity Mn^{2+} and Mg^{2+} experiments had to be carried out at different pH values, and pH-dependent effects cannot be ruled out. When Mn^{2+} was supplied as the cofactor for the EcoRV-catalyzed reaction of plasmid substrates, addition of calcium ions stimulated or first stimulated then inhibited reactions (23). This was explained by the formation of a mixed enzyme $Mn^{2+}Ca^{2+}$ species that was more reactive than an $Mn^{2+}Mn^{2+}$ form. However, a detailed study at low concentrations of Ca^{2+} revealed that no stimulation of activity was observed in the Mn^{2+}-supported FEN reaction (Fig. 2*b*).

$$\frac{k_{obs}}{k_0} = \frac{K_i}{K_i + [Ca^{2+}]} \quad \text{(Eq. 7)}$$

The observation that the overall FEN reaction requires the presence of at least three magnesium ions (Fig. 2*c*) suggests that a competitive inhibition scheme based on binding one Ca^{2+} ion (Equation 7) could be too simplistic as the calcium ions could replace more than one of the viable cofactor ions. Evidence that this is the case is observed at higher concentrations of inhibitory ions, where the Ca^{2+} dependence deviates from that predicted from a simple competitive inhibition model (Equation 7). In these regions, the slopes of log-log plots are −2.0 ± 0.1 (0.1 mM Mn^{2+}) and −2.1 ± 0.2 (2 mM Mg^{2+}) rather than the slope of −1 predicted by the simple competitive inhibition model (Fig. 3, *b* and *c*). Thus the simultaneous binding of two calcium ions inhibits the FEN reaction. However, a model where the presence of two calcium ions is the sole inhibitory form of the enzyme-substrate complex is also inadequate as this would give rise to a slope of −2 over the entire Ca^{2+}-dependent data range. Assuming that Ca^{2+} ions inhibit the reaction by displacing catalytically competent cofactors, the FEN protein

must possess at least two viable cofactor ions at specific sites, and replacement of either or both of these by Ca^{2+} significantly reduces activity. However, it is possible that one of the three FEN metal ions can be replaced by Ca^{2+} without altering the ability to catalyze the reaction. A similar biphasic response to inhibitory Ca^{2+} ions has been noted for the magnesium-supported reactions of the *Tetrahymena* ribozyme (24).

DISCUSSION

The data presented here demonstrate that the overall T5FEN-catalyzed reaction requires at least three magnesium ions. However, most FEN x-ray structures (in the absence of substrate) show only two divalent metal ions bound (Fig. 1*b*), consistent with ITC studies of divalent metal ion binding to T5FEN (12). This implies that a third metal ion binds in the presence of substrate and has a lower association constant for the free enzyme. There are several structural precedents for the binding of additional active site metal ions by nucleases in the presence of substrate or products. A recent example is RNase HI where x-ray crystallography revealed the presence of a single magnesium ion in the absence of substrate (25), but an inhibited enzyme-nucleic complex contained two active site magnesium ions (26). However, debate has focused on the functional relevance of the metal ions within co-crystal structures and whether these additional metal ions are required for catalysis of phosphate diester hydrolysis.

For the T5FEN reaction, the magnesium ion response of the maximal FEN reaction rate (k_{cat} or k_{ST}) requires at least two independently bound magnesium ions. The calcium ion inhibition data also provide evidence for two inhibitory metal ion binding sites. This is most simply explained by a competitive inhibition scheme where replacement of either or both of the catalytically essential viable cofactors leads to inactivation. The finding that at least two viable cofactor ions are required to render the FEN protein catalytically competent makes it plausible that FEN derives its major rate acceleration using a two-metal-ion mechanism. This mechanism involves two metal ions interacting with the same oxygen atom of the scissile phosphate diester and requires they must have a separation of $\leq$4 Å (Fig. 1*a*). The separation of the two metal ions (designated metal 1 and 2) observed in the T5FEN structure (8 Å) is much greater than this (Fig. 1*b*). However, in one hFEN structure two metal ions are liganded with a separation of 3.4 Å (Fig. 1*b* and supplemental Fig. S1) (15) to the same central carboxylate of the FEN active site, in an analogous fashion to the metal ion coordination observed in other nucleases (3, 26). The third T5FEN metal ion (metal 3), implicated by this study, could bind to Asp-130 in close proximity to metal 1 in an analogous fashion to the metal coordination observed in hFEN, and support a two-metal-ion mechanism for chemical catalysis. Mutation of Asp-130, or its equivalent in other FENs, leads to undetectable activity, supporting a key role for this Asp-130 site in metal ion coordination (12, 27, 28). In contrast mutation of metal 2 coordinating carboxylates in T5FEN produces readily detectable activity (12), suggestive metal 2 does not play a vital role in catalysis. Superposition of hFEN and T5FEN structures demonstrate that the third metal ion implicated by this study could be accommodated within the T5FEN active site bound to Asp-130 to support a two metal ion mechanism (Fig. 1*b*). However, the possibility remains that metal ions not involved in direct scissile bond interactions could contribute substantive rate acceleration by transition state stabilization (29) and the location of the third metal ion required by the T5FEN reaction merits further investigation.

Metal ions involved in the overall FEN catalytic process could potentially play roles in substrate binding equilibria and/or chemical catalysis. Therefore, this study provides evidence that between one and three ions could participate in FEN substrate equilibria as the overall FEN reaction has a three metal ion requirement. The magnesium ion dependence of $1/K_m$ can only be explained by the participation of at least two ions. For enzyme reactions rate limited by steps other than the chemical reaction under steady state conditions, K_m values define the concentration of substrate required to convert half the enzyme into the form(s) proceeding the rate-limiting step(s) (30). As product release is partially rate-limiting for the WT T5FEN-catalyzed reaction of HP5F ($k_{ST} = 2.3\ k_{cat}$), the stability of enzyme-product species is measured by K_m. Furthermore, the stability of any intermediates formed after initial interaction of enzyme and substrate would also be reflected in this parameter. In the absence of direct interrogation of all of these enzyme-substrate and enzyme-product equilibria, any interpretation of the metal ion dependence of $1/K_m$ is tentative, but the data suggest a role for metal ions in stabilizing T5FEN-substrate equilibria.

Support for a requirement for metal ion(s) for productive substrate binding is provided by a recent bacteriophage T4FEN structure solved in complex with pseudo-Y DNA (8). This structure lacks divalent metal ions and has a mutation of metal 1-liganding central carboxylate (D132N). The DNA substrate makes no contacts with the FEN active site lacking metal ions, presumably due to the electrostatic repulsion by the carboxylates. Thus, bound metal ion(s) are probably required to stabilize a FEN-DNA complex where substrate is positioned for reaction to occur.

An intriguing feature of the T4FEN DNA structure is that the scissile phosphate corresponding to the major site of FEN reaction, one nucleotide into the duplex region at the site of bifurcation, is located within duplex DNA bound parallel to the active site. Positioning metal 1 within the T4-DNA complex according to a T4FEN structure without substrate bound (9) placed this ion 7 Å away from this scissile phosphate (8) (supplemental Fig. S4*b*). Metal 2 is at a much greater distance from the major reaction site (8). Nevertheless, a model of T5FEN-DNA interaction, based upon overlay with the T4-DNA structure, is in excellent agreement with experimental data on the interactions of the protein with the duplex and the 3′-overhang of the pseudo-Y (supplemental Fig. S4*a*) (19, 31). This makes it difficult to envisage how the scissile phosphate, one nucleotide into the duplex region, can bind within the active site while still maintaining a Watson-Crick terminal base pair and the functional substrate-protein contacts. However, breaking the terminal base pair and making at least the first nucleotide and reaction site extrahelical would allow active site binding while maintaining substrate-protein contacts. The metal dependence of substrate equilibria observed here may be the consequence of a metal dependent conformational change, analogous to the

nucleotide flipping seen in base excision repair enzymes (32), which positions the scissile bond within the active site (supplemental Fig. S4*c*).

The reactions of all FENs may have an overall three metal ion requirement. However, in archaeal and hFEN structures (10, 14–17) the protein N terminus occupies a position similar to metal ion 2 in phage enzymes (supplemental Fig. S1). In bacteriophage and bacterial FEN structures, this region is disordered (7, 9, 13). Bacteriophage FENs lacking the N-terminal regions possess wild type activity (12, 33), whereas the functional relevance of the N-terminal region of archaeal and mammalian FENs is untested. It is possible that the N terminus might substitute for metal ion 2 in these enzymes. While the role played by metal 2 deserves further investigation it could act in stabilization of FEN-substrate equilibria and/or may play a non-essential but rate accelerating role in chemical catalysis. It is intriguing to note that the same function may be provided by the protein in higher organism FENs.

Other phosphoryl transferases have three metal ion active sites. For phosphate diesterases that contain three active site zinc ions, such as nuclease P1 (34), phospholipase C (35, 36), and endonuclease IV (37, 38), all three metals are suggested to act in chemical catalysis, but different mechanisms involving these three metal ions have been proposed. Several magnesium-dependent nucleases with three metal ion binding sites may also exist, such as the group I intron (39), EcoRV (40), and 3′-5′ exonuclease (41). Even the prototype two-metal-ion mechanism phosphoryl transferase, the phosphate monoesterase alkaline phosphatase, has an active site composed of two zinc ions plus one magnesium ion, and magnesium ions stimulate activity (2). Thus our new results on T5FEN in the context of existing data argue that three metal ion active sites may be a more common phenomena than previously suspected. Additional metal ions could influence biological efficacy by either moderating chemical reactivity or physical steps of the catalytic cycle such as substrate association, conformational changes, and enzyme-product stability. Thus, while a mechanism can be envisaged for rate accelerations of phosphate monoesterases and diesterases involving two metal ions, the biological function of other phosphoryl transferases in DNA replication, DNA repair, RNA processing, and RNA degradation may well involve a third ion or its functional equivalent.

Acknowledgments—We thank Elaine Frary for technical assistance, Alan Cox for recording the ICP mass spectra, and Hal Dixon (Cambridge) and Structural Cell Biology of DNA Repair (SBDR) members for discussions.

REFERENCES

1. Schroeder, G. K., Lad, C., Wyman, P., Williams, N. H., and Wolfenden, R. (2006) *Proc. Natl. Acad. Sci. U. S. A.* **103,** 4052–4055
2. Kim, E. E., and Wyckoff, H. W. (1991) *J. Mol. Biol.* **218,** 449–464
3. Beese, L. S., and Steitz, T. A. (1991) *EMBO J.* **10,** 25–33
4. Sigel, R. K. O., and Pyle, A. M. (2007) *Chem. Rev.* **107,** 97–113
5. Yang, W., Lee, J. Y., and Nowotny, M. (2006) *Mol. Cell* **22,** 5–13
6. Pingoud, A., Fuxreiter, M., Pingoud, V., and Wende, W. (2005) *Cell. Mol. Life Sciences* **62,** 685–707
7. Kim, Y., Eom, S., Wang, J., Lee, D., Suh, S., and Steitz, T. (1995) *Nature* **376,** 612–616
8. Devos, J. M., Tomanicek, S. J., Jones, C. E., Nossal, N. G., and Mueser, T. J. (2007) *J. Biol. Chem.* **282,** 31713–31724
9. Mueser, T. C., Nossal, N. G., and Hyde, C. C. (1996) *Cell* **85,** 1101–1112
10. Hosfield, D. J., Mol, C. D., Shen, B. H., and Tainer, J. A. (1998) *Cell* **95,** 135–146
11. Zheng, L., Li, M., Shan, J. X., Krishnamoorthi, R., and Shen, B. H. (2002) *Biochemistry* **41,** 10323–10331
12. Feng, M., Patel, D., Dervan, J. J., Ceska, T., Suck, D., Haq, I., and Sayers, J. R. (2004) *Nat. Struct. Mol. Biol.* **11,** 450–456
13. Ceska, T. A., Sayers, J. R., Stier, G., and Suck, D. (1996) *Nature* **382,** 90–93
14. Hwang, K. Y., Baek, K., Kim, H. Y., and Cho, Y. (1998) *Nat. Struct. Biol.* **5,** 707–713
15. Sakurai, S., Kitano, K., Yamaguchi, H., Hamada, K., Okada, K., Fukuda, K., Uchida, M., Ohtsuka, E., Morioka, H., and Hakoshima, T. (2005) *EMBO J.* **24,** 683–693
16. Matsui, E., Musti, K. V., Abe, J., Yamasaki, K., Matsui, I., and Harata, K. (2002) *J. Biol. Chem.* **277,** 37840–37847
17. Chapados, B. R., Hosfield, D. J., Han, S., Qiu, J. Z., Yelent, B., Shen, B. H., and Tainer, J. A. (2004) *Cell* **116,** 39–50
18. Sayers, J. R., and Eckstein, F. (1990) *J. Biol. Chem.* **265,** 18311–18317
19. Williams, R., Sengerová, B., Osborne, S., Syson, K., Ault, S., Kilgour, A., Chapados, B. R., Tainer, J. A., Sayers, J. R., and Grasby, J. A. (2007) *J. Mol. Biol.* **371,** 34–48
20. Pickering, T. J., Garforth, S. J., Sayers, J. R., and Grasby, J. A. (1999) *J. Biol. Chem.* **274,** 17711–17717
21. Tock, M. R., Frary, E., Sayers, J. R., and Grasby, J. A. (2003) *EMBO J.* **22,** 995–1004
22. Patel, D. V., Tock, M. R., Frary, E., Feng, M., Pickering, T. J., Grasby, J. A., and Sayers, J. R. (2002) *J. Mol. Biol.* **320,** 1025–1035
23. Vipond, I. B., Baldwin, G. S., and Halford, S. E. (1995) *Biochemistry* **34,** 697–704
24. McConnell, T. S., Herschlag, D. M., and Cech, T. R. (1997) *Biochemistry* **36,** 8293–8303
25. Yang, W., Hendrickson, W. A., Crouch, R. J., and Satow, Y. (1990) *Science* **249,** 1398–1405
26. Nowotny, M., Gaidamakov, S. A., Crouch, R. J., and Yang, W. (2005) *Cell* **121,** 1005–1016
27. Bhagwat, M., Meara, D., and Nossal, N. G. (1997) *J. Biol. Chem.* **272,** 28531–28538
28. Shen, B. H., Nolan, J. P., Sklar, L. A., and Park, M. S. (1997) *Nucleic Acids Res.* **25,** 3332–3338
29. Amyes, T. L., Richard, J. P., and Tait, J. J. (2005) *J. Am. Chem. Soc.* **127,** 15708–15709
30. Gutfreund, F. (1995) *Kinetics for the Life Sciences*, Cambridge University Press, Cambridge
31. Dervan, J. J., Feng, M., Patel, D., Grasby, J. A., Artymiuk, P. J., Ceska, T. A., and Sayers, J. R. (2002) *Proc. Natl. Acad. Sci. U. S. A.* **99,** 8542–8547
32. Hitomi, K., Iwai, S., and Tainer, J. A. (2007) *DNA Repair (Amst).* **6,** 410–428
33. Gangisetty, O., Jones, C., Bhagwat, M., and Nossal, N. (2005) *J. Biol. Chem.* **280,** 12876–12887
34. Volbeda, A., Lahm, A., Sakiyama, F., and Suck, D. (1991) *EMBO J.* **10,** 1607–1618
35. Hough, E., Hansen, L. K., Birknes, B., Jynge, K., Hansen, S., Hordvik, A., Little, C., Dodson, E., and Derewenda, Z. (1989) *Nature* **338,** 357–360
36. Hansen, S., Hough, E., Svensson, L. A., Wong, Y. L., and Martin, S. F. (1993) *J. Mol. Biol.* **234,** 179–187
37. Hosfield, D. J., Guan, Y., Haas, B. J., Cunningham, R. P., and Tainer, J. A. (1999) *Cell* **98,** 397–408
38. Garcin, E. D., Hosfield, D. J., Desai, S. A., Haas, B. J., Björas, M., Cunningham, R. P., and Tainer, J. A. (2008) *Nat. Struct. Mol. Biol.* **15,** 515–522
39. Shan, S. O., Yoshida, A., Sun, S. G., Piccirilli, J. A., and Herschlag, D. (1999) *Proc. Natl. Acad. Sci. U. S. A.* **96,** 12299–12304
40. Horton, N. C., and Perona, J. J. (2004) *Biochemistry* **43,** 6841–6857
41. Han, H., Rifkind, J. M., and Mildvan, A. S. (1991) *Biochemistry* **30,** 11104–11108